# Scattering of High-Energy Positrons from Protons*

D. YOUNT† AND J. PINE
*High-Energy Physics Laboratory, Stanford University, Stanford, California*
(Received June 25, 1962)

Positron and electron beams from the Stanford Mark III linear accelerator have been used to investigate the importance of two-photon exchanges in electron scattering from the proton. The scattering cross sections for positrons and electrons have been compared at 200 and 300 MeV for $q^2$ (the square of the four-momentum transfer) from 0.3 to 5.2 $F^{-2}$. The results show no evidence of anomalous two-photon effects and verify the correctness of the first Born approximation form factor analysis to within a few percent or better for this range of $q^2$. The variation of the cross sections with $q^2$ has also been measured with high accuracy.

The specific ionizations of 300-MeV positrons and electrons in hydrogen at one atmosphere have been compared in the course of the experiment, and found to be equal to within $\pm 0.3\%$.

## I. INTRODUCTION

THE importance of two-photon exchanges in electron scattering from the proton can be determined by comparing electron and positron elastic scattering cross sections. Figure 1 shows the Feynman diagrams involved, to order $\alpha^3$. Diagram 1 of Fig. 1 alone leads to the familiar Rosenbluth cross section and to the usual form factor analysis. The higher-order diagrams are expected to manifest themselves through interference with diagram 1. If electrons are replaced by positrons, the sign of the interference terms involving diagrams 2 and 3 is reversed. Thus, a comparison of positron and electron scattering (at identical angles and energies) may be used to measure these two-photon exchanges. The effect of the other second-order diagrams is small, and identical for positrons and electrons.

If the proton is considered to be a rigid charge and moment distribution, then the two-photon exchanges represent the distortion of the electron wave function by the proton's field. At the energies and angles of this experiment, this effect has been estimated by Yennie, Lévy, and Ravenhall[1] to change the cross section by

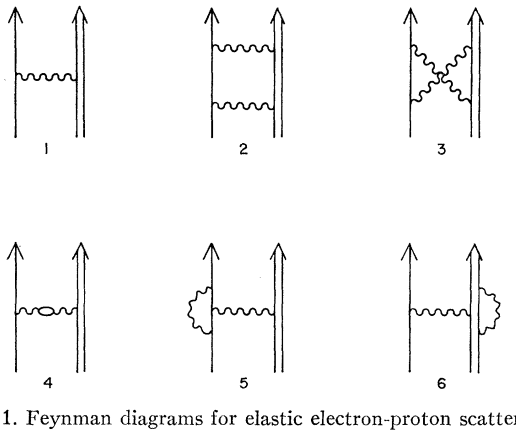


FIG. 1. Feynman diagrams for elastic electron-proton scattering.

$\lesssim 0.25\%$. When a dynamical proton structure is assumed, two-photon effects may also result from proton polarizability. This may be visualized as arising from the excitation of virtual isobaric states (corresponding, for example, to resonances in pion photoproduction). Polarizability has been estimated to influence the cross section by $\lesssim 1\%$ in the region explored here,[2-4] but such estimates involve meson physics and are, of necessity, approximate.

This experiment was motivated by the importance of nuclear structure determinations and by the possibility that unexpectedly large two-photon effects might be found. In such a case, the analysis based on the Rosenbluth formula would be misleading. The quantity determined here is $R$, defined by

$$R \equiv (\sigma_- - \sigma_+)/(\sigma_- + \sigma_+),$$

where $\sigma_-$ and $\sigma_+$ are the differential scattering cross sections for electrons and positrons at identical angles and energies. There is a contribution to $R$ which arises from the radiative corrections if proton recoil is considered. The radiative corrections calculated by Tsai[5] include this effect and predict corrections to $R$ of $\lesssim 0.01$ for this experiment.

## II. APPARATUS

A schematic view of the Stanford Mark III accelerator is shown in Fig. 2. Electrons were accelerated from the gun to a tantalum radiator of thickness 3.2 radiation lengths, where they produced positrons by pair production from bremsstrahlung gamma rays. The remainder of the accelerator was used to accelerate the many low-energy ($\sim 10$ MeV) positrons emerging from the radiator. This was easily done by introducing a phase shift of 180° in the rf power fed to this part of the machine. The beam was momentum analyzed by the double-deflection magnet system; and, for $\pm 1\%$ momentum spread, intensities of up to $7 \times 10^6$ positrons per pulse (60 pulses per sec) were obtained at 300 MeV.

* This work was supported in part by the Office of Naval Research, the U. S. Atomic Energy Commission, and the Air Force Office of Scientific Research.

† Now at the Department of Physics, Princeton University, Princeton, New Jersey.

[1] D. Yennie, M. Lévy, and D. G. Ravenhall, Revs. Modern Phys. **29**, 144 (1957).

[2] S. D. Drell and M. Ruderman, Phys. Rev. **106**, 561 (1957).

[3] S. D. Drell and S. Fubini, Phys. Rev. **113**, 741 (1959).

[4] N. R. Werthamer and M. A. Ruderman, Phys. Rev. **123**, 1005 (1961).

[5] Y. S. Tsai, Phys. Rev. **122**, 1898 (1961).

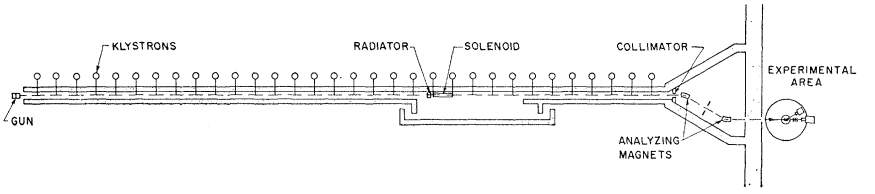


FIG. 2. Schematic drawing of the Stanford Mark III Accelerator.

This was a factor of about 5000 less than the usual electron beam current. The positron production techniques have been described in more detail elsewhere.[6] Electrons were obtained by withdrawing the radiator and leaving the phasing unchanged so that electrons were accelerated to 600 MeV and then decelerated to 300 MeV. Electrons and positrons at 200 MeV were obtained by turning off some of the klystrons.

The field of the momentum-analyzing magnet was monitored with a rotating coil fluxmeter of the type described by Bumiller *et al.*[7] The output leads from the coil were reversed in changing beams so that the balancing potentiometer of the coil electronics had the same setting for electrons and positrons. Under these conditions the magnetic field was reversible to better than $\pm 0.1\%$. Identical momentum slit settings ($\pm 1\%$) were used for electron and positron beams, and their mean energies were very closely equal. Factors leading to small energy differences are discussed in Sec. III. The vertical positions of the beams at the target were controlled by a set of Helmholtz coils located in front of the analyzing system. Horizontal steering was done by unbalancing the second magnet relative to the momentum-analyzing magnet. Neither type of steering influences the beam energy.

Figure 3 shows the apparatus in the experimental area. The target contained liquid hydrogen in a cell 2-in.$\times$2-in. in cross section and 8 in. long in the direction of the beam. The beam centering at the target was monitored continuously with a "beam sniffer." This was a hydrogen-filled ion chamber with two 0.001-in. aluminum collector plates oriented perpendicular to the beam direction. Each of the plates was split into two halves by a narrow gap, horizontal in one case and vertical in the other. The ion currents from the two halves of a given collector were amplified by matched dc amplifiers. The beam was steered so that the outputs were equal to within $\pm 20\%$. In this manner the beam was centered at the crossed gaps to an accuracy of $\pm 0.025$ in. X-ray films were exposed to check the beam position and to determine the beam shape. The "sniffer" was always found to be functioning properly, and the shapes of positron and electron beams were very similar.

The primary beam current monitor was the "300-MeV" Faraday cup described by Brown and Tautfest,[8] with several modifications. The entrance snout had been extended by about 10 in.; the system of permanent magnets at the bottom of the cup had a field of 60 G instead of 300 G; and the thickness of the cup along the beam had been increased by about 8 in. of iron.

Two hydrogen-filled ion chambers were used simultaneously as secondary monitors. These were similar to the "beam sniffer" except that in each a single nonsplit collecting plate was used. The gas was flowing through one (the "flow" chamber) at a few cubic feet per hour while the other (the "closed" chamber) was sealed off. The efficiencies of the two chambers were independent of beam intensity to $\pm 0.1\%$ for beam currents up to $10^8$ and $10^7$ particles per pulse, respectively (the difference being due presumably to the lower purity of the hydrogen in the closed chamber). The pressure in the flow chamber was maintained at 1-mm mercury above atmospheric pressure by means of a bubbler, and the gas gain of this chamber was corrected for measured changes in temperature and barometric pressure. The closed chamber was at approximately 2 psi above atmospheric pressure. Any significant variation in the gain of either chamber or of its electronic integrator was expected to show up in the ratio of the two outputs. The charge collected by the ion chambers, as well as by the Faraday cup, was integrated with slide back integrators which had long-time accuracy of better than $\pm 0.1\%$ and random short-time fluctuations of about $\pm 0.2\%$.

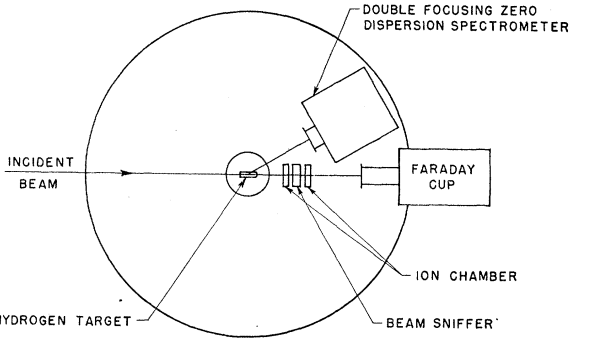


FIG. 3. Experimental layout.

[6] D. Yount and J. Pine, Nuclear Instr. and Methods **15**, 45 (1962).

[7] F. A. Bumiller, J. F. Oeser, and E. B Dally, *Proceedings of the International Conference on Instrumentation in High-Energy Physics at Berkeley, California, 1960* (Interscience Publishers, Inc., New York, 1961), p. 308.

[8] K. L. Brown and G. W. Tautfest, Rev. Sci. Instr. **27**, 696 (1956). [See also F. A. Bumiller and E. B. Dally, *Proceedings of the International Conference on Instrumentation in High-Energy Physics at Berkeley, California, 1960* (Interscience Publishers, Inc., New York, 1961), p. 305.]

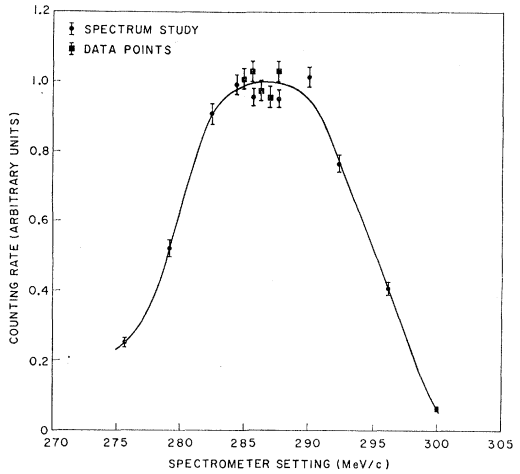


FIG. 4. Counting rate vs spectrometer setting for electrons at 30°, 300 MeV.

The double-focusing zero-dispersion magnetic spectrometer described by Alvarez *et al.*[9] was used to select the energies and angles of scattered electrons and positrons. Data were taken at right and left scattering angles. The spectrometer angles were reproduced to better than $\pm 0.001°$ by using dial indicators or sliding electrical contactors to establish the magnet position relative to fixed reference blocks anchored to the floor of the experimental area. The spectrometer field was monitored by a rotating coil of a different type from that used in the momentum-analyzing magnet, with reversibility also better than $\pm 0.1\%$.

The scattered electrons and positrons were detected by two plastic scintillators, $\frac{1}{4}$ in. thick and $4\frac{1}{2}$ in. in diameter, used in coincidence. The zero-dispersion spectrometer optics caused all particles to pass well away from the edges of the scintillators. The counter electronics was operated extremely conservatively; and tests, such as changing the phototube gains to half or twice the operating values, did not affect the counting efficiency within statistical errors of $\pm 1\%$. No observable change in phototube gain resulted from reversing the spectrometer field.

## III. DATA, CORRECTIONS, AND UNCERTAINTIES

### Procedure

The ratio $R$ was measured for four points: 205 MeV, 30°; and 307 MeV, 30°, 45°, and 130°, where incident energies and angles are given in the laboratory system. The energies are uncertain by about $\pm 1\%$; their precise value is of little consequence for the data on $R$, and in the text nominal values of 200 and 300 MeV have generally been used.

A determination of $R$ included the following procedures:

1. Intercalibration of ion chambers with the Faraday cup.
2. Determination of the scattered energy with the spectrometer, as a check against the analyzing magnets.
3. Measurement of the yield of scattered electrons at three to six slightly different spectrometer field settings, equally spaced over a momentum interval of 0.4% to 1.0% centered at the peak of the scattered spectrum.
4. Measurement of right and left scattering for each spectrometer momentum setting.
5. Measurement of empty target background for right and left scattering at the center of the momentum interval covered in 3.
6. Intercalibration of the ion chambers with the Faraday cup. (During the measurements, the Faraday cup was removed from the beam line to allow rapid angle cycling and, in the case of the 130° point, to reduce background.)
7. Photographing of the beam on x-ray film placed directly in front of the target.
8. Repetition of steps 1–7 for positrons.

Procedures 3 and 4 were intermixed, while 5 and 7 took place near the beginning or end of the sequence. The beam position was monitored continually with the "sniffer" ion chamber, and very thorough checks of the counters and beam integrators were performed at the beginning of each run. For the point at 300 MeV, 130°, angle cycling was not used, nor were data taken at more than one spectrometer setting. The low statistical accuracy obtainable in this case made these procedures superfluous. Although the sequence above refers to data for electrons preceding that for positrons, the inverse order was used about as often.

The spectrometer was set to accept a momentum range of 7% in order to minimize effects of the 2% momentum spread of the incident beam, the radiative corrections, and any small drifts in the magnetic fields of the spectrometer and analyzing magnets. Figure 4 shows a typical "spectrum" (counting rate plotted as a function of spectrometer field). Data were taken in a small region centered on the flat peak, while the edges of the spectrum provided an energy measurement with a precision of $\pm 0.1\%$. (See procedure, step 2.)

The solid angle accepted by the spectrometer was about 0.004 sr, defined by a tapered entrance collimator, while the target length seen by the spectrometer was 2 to 4 in., depending on the scattering angle. The target entrance and exit windows were outside the field of view of the spectrometer, and the empty target counting rates were in all cases consistent with scattering from residual hydrogen gas in the target.

In determining $R$, counting rates for right and left scattering were averaged to eliminate errors due to changes in beam direction. Furthermore, the integrated beam was obtained by averaging results given by the three monitors. Column 3 of Table I gives $R_0$, the value of $R$ determined from the averages just mentioned,

[9] R. A. Alvarez, K. L. Brown, W. K. H. Panofsky, and C. T. Rockhold, Rev. Sci. Instr. **31**, 556 (1960).

TABLE I. Values of $R$, corrections ($\delta_i$), and uncertainties ($\epsilon_i$). Briefly, the subscripts have the following significance: stat = statistical, M = monitor, E = energy, r = counting losses, T = Tsai (radiative correction), and sp = spectrum. $R_0$ is the observed value of $R$ corrected only for counting rate losses, while $R_F$ and $\epsilon_F$ are, respectively, the final corrected value of $R$ and the final experimental standard error in $R$.

| 1 Energy (MeV) | 2 Angle (deg) | 3 $R_0$ | 4 $\epsilon_{stat}$ | 5 $\epsilon_M$ | 6 $\delta_E$ | 7 $\epsilon_E$ | 8 $\epsilon_r$ | 9 $\delta_T$ | 10 $\epsilon_{sp}$ | 11 $R_F$ | 12 $\epsilon_F$ |
|---|---|---|---|---|---|---|---|---|---|---|---|
| 205 | 30 | +0.003 | ±0.005 | ±0.002 | −0.002 | ±0.002 | ±0.001 | +0.001 | ±0.002 | +0.002 | ±0.006 |
| 307 | 30 | +0.009 | ±0.007 | ±0.002 | +0.002 | ±0.002 | ±0.001 | +0.001 | ±0.002 | +0.012 | ±0.008 |
| 307 | 30 | −0.004 | ±0.008 | ±0.002 | +0.000 | ±0.002 | ±0.001 | +0.001 | ±0.002 | −0.003 | ±0.009 |
| 307 | 45 | −0.005 | ±0.015 | ±0.002 | +0.000 | ±0.003 | ±0.000 | +0.003 | ±0.002 | −0.002 | ±0.016 |
| 307 | 130 | −0.029 | ±0.029 | ±0.003 | −0.003 | ±0.005 | ±0.000 | +0.011 | ±0.005 | −0.021 | ±0.030 |

while column 4 gives $\epsilon_{stat}$, the purely statistical uncertainty in $R_0$. The remainder of the table lists the corrections and uncertainties discussed below, with final values of $R$ given in column 11 and final uncertainties in column 12. Two determinations of $R$ at 30°, 300 MeV which were widely separated in time, are shown separately in the table.

## Beam Monitors

Any systematic monitor bias depending on whether a positron or electron beam is being used will, of course, lead directly to an error in $R$. The beam intensities and shapes were sufficiently similar so that no significant effects arose from variations in these parameters. The asymmetry in electron-electron scattering as compared with positron-electron scattering raises the question of a possible bias associated with the different numbers of knock-on electrons from the material in front of the monitors. The fact that knock-ons subtract from the beam charge for positrons and add for electrons will also affect the Faraday cup efficiency. These effects have been calculated and were found to be negligible.

We know of no detailed calculations for the difference in specific ionization for positrons and electrons in hydrogen, although there is no reason to expect a significant effect. This difference has been treated as an unknown to be determined by comparison of the ion chambers with the Faraday cup. Data reported in the Appendix indicate that the Faraday cup bias (difference in efficiency for positrons and electrons) was less than ±0.3%. This introduces an uncertainty in $R$ of ±0.0015. Intercalibrations of the ion chambers with the Faraday cup for eleven changes in the sign of the beam indicate that the ion chamber and Faraday cup biases were identical to ±0.1%. The combined monitor data thus establish the equality of the specific ionizations of positrons and electrons in hydrogen to ±0.3%.

The monitors exhibit random fluctuations evidenced by variations in the ratios of the outputs of the three monitors. The uncertainty in $R$ arising from these fluctuations is given in column 5 of Table I. It has been calculated in two ways: from the mean standard deviation for a single monitor reading as determined from the many monitor ratios obtained during the experiment, and from the fluctuations in the several monitor ratios for the particular point involved. The assigned uncertainty is the larger of the two estimates. The uncertainty in $R$(±0.0015) which arises from the possible systematic monitor bias is not shown in Table I. It would shift all points equally, by an amount small compared with the final estimated uncertainties.

## Angle

In changing from electrons to positrons, the field of the momentum-analyzing magnet of the double-deflection system was accurately reversed. The beam was then steered horizontally to center it at the "beam sniffer" ion chamber. This was done by varying the current in the second magnet of the system. Merely reversing the fields in both magnets does not, in general, produce identical electron and positron trajectories, nor are the paths identical after the steering just described. The main reason for the differences in trajectory is the fact that positron and electron beams emerge from the accelerator at slightly different angles and positions.

Under the conditions of this experiment, the center of gravity of the beam at the end of the accelerator may vary by about ±$\frac{1}{8}$ in., while the beam direction can change by about ±0.001 rad. Such differences can arise from extreme changes in accelerator operating conditions and can give rise to changes in beam direction at the target of about ±0.1 degree. If data were taken only on the right or on the left of the beam path, this angular variation would introduce a significant error in $R$ for small scattering angles. Averaging measurements of right and left scattering cancels this error to first order, while the measured right-left asymmetry can be used to determine the difference in angle and correct the error to higher order. Higher order correction has not been necessary, but the observed asymmetries verify the presence of angle differences which were consistent with the estimate above. For a given electron or positron beam the angle was very stable, with differences occurring between different beams.

The final uncertainty in $R$ arising from angle errors is estimated to be less than ±0.001, including the uncertainty in setting the spectrometer angles. This uncertainty is so small that it has been neglected.

### Energy

A number of factors have been considered in estimating possible differences in incident electron and positron energies. These include: rotating coil and current regulator performance; hysteresis effects which change the integral of the field along the trajectory through the momentum-analyzing magnet; energy spectra, *angles*, and *positions* of the beams at the collimator before entering the analyzing system; and *stray fields* (e.g., the earth's magnetic field). The factors in italics lead to differences in beam direction at the target, which give rise to the observed differences in the left-right asymmetries for positrons and electrons. The possibility of measuring and perhaps reducing the energy error is thus a useful by-product of the angle cycling procedure.

In calculating the differences in beam directions from the left-right asymmetries, a distinction must be made between thin targets and the present extended target whose active length is defined by the spectrometer. In the first case, beam displacements at the target also lead to changes in the scattering angle and thus in the left-right asymmetries, while in the second case, only the directions of the beams are important. (Small changes in the active target length and in the solid angle of the spectrometer lead to negligible asymmetries.) As far as the errors in angle are concerned, angle cycling is effective in either case.

The energy difference can be computed from the measured difference in beam directions at the target and from the known optical properties of the analyzing system.[10] Depending upon the accuracy with which the beams are centered at the "beam sniffer" and the uncertainties (primarily statistical) in the left-right asymmetries, limits on the energy difference may be established which are either more or less precise than those based on *a priori* estimates of trajectory uncertainties. For the data reported here, the left-right asymmetries, while consistent with the *a priori* estimates, allow no significant reduction in the uncertainty in $R$ due to possible energy differences. However, useful corrections have been determined with this method and have been used in analyzing results on the scattering of electrons and positrons from cobalt and bismuth.[11]

A second test of the energies is provided by the spectrometer. The accuracy of this measurement was limited primarily by the statistical errors of the measured spectra, since the systematic error for this instrument under the present experimental conditions was $\pm 0.1\%$. The energy corrections shown in column 6 of Table I are based on the weighted average of the determinations of the spectrometer and of the momentum analyzing system. The energy error of column 7 is dominated by an uncertainty computed by treating the two values as independent measurements having random errors. Energy uncertainties from all sources listed at the beginning of this section, and estimated systematic uncertainties of the spectrometer, are included in the error shown in column 7.

### Miscellaneous Uncertainties

Since the dead time of the scalers which were used in the experiment was longer than the beam pulse, counting rate losses depended only upon the charge per pulse and not upon the instantaneous current. A rate correction based on the mean charge per pulse may be in error as a result of pulse-to-pulse fluctuations or secular changes in beam intensity during the counting period. The experimental conditions permitted particularly stable accelerator operation which reduced fluctuations to a minimum, while the cycling procedures, with correspondingly short integrating periods ($\sim$10 min), provided a strong check against secular changes of all kinds.

A likely estimate of the uncertainty in the counting rate corrections (believed to represent a "standard deviation") was made by computing the correction for equal numbers of beam pulses of two sizes in the ratio 1.5:1 and comparing this to the result for uniform pulses. For the nonuniform case the correction is about 1.04 times as great. Since electron and positron rates were closely equal, a symmetrical error has been assigned in $R$ based on a 4% uncertainty in the net rate correction. This is given in column 8 of Table I, while the rate correction itself has been taken into account in the values for $R_0$.

Radiative corrections were calculated from the formula given by Tsai[5] with $\Delta E/E_0=3\%$, where $\Delta E$ is the maximum energy which a positron or electron can radiate and still be accepted by the spectrometer, and $E_0$ is the incident energy. The Tsai correction to $R$ is shown in column 9 of Table I. The uncertainty associated with this correction was determined con-

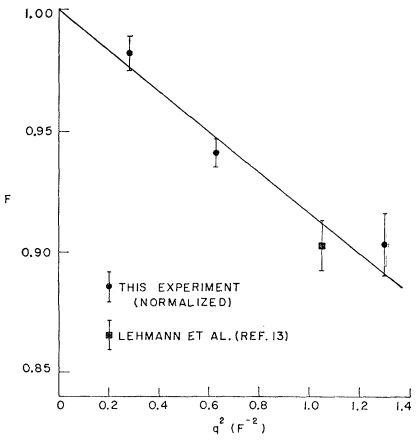


FIG. 5. Variation of the proton form factor $F$ with $q^2$. The straight line is the low-$q$ approximation for an rms radius equal to 0.72 F.

[10] K. L. Brown, Rev. Sci. Instr. **27**, 959 (1956).
[11] J. Goldemberg, J. Pine, and D. Yount (to be published).

TABLE II. Electron-proton scattering cross sections and the squared form factors $F^2$. The standard error in both quantities is given, but does not include an over-all normalization uncertainty of ±1.5%.

| 1 Energy (MeV) | 2 Angle (deg) | 3 $q^2$ $(F)^{-2}$ | 4 $d\sigma/d\Omega$ (cm²/sr) | 5 $F^2$ | 6 Standard error (%) |
|---|---|---|---|---|---|
| 205 | 30 | 0.281 | $2.43\times10^{-29}$ | 0.965 | ±1.4 |
| 307 | 30 | 0.624 | $9.93\times10^{-30}$ | 0.885 | ±1.1 |
| 307 | 45 | 1.30 | $1.75\times10^{-30}$ | 0.816 | ±2.9 |
| 307 | 130 | 5.2 | $2.01\times10^{-31}$ | 0.416 | ±4.8 |

servatively from the variation for $\Delta E/E_0=2\%$ and 5%, and is negligible.

A "spectrum" error was assigned corresponding to uncertainties in the relative centering of positron and electron points on their respective elastic peaks. Owing to the flatness of the spectrometer response and to the accuracy of the energy determinations, this error, given in column 10 of Table I, was small. Positron and electron spectra were indistinguishable, as expected.

The net effect of positron annihilation in flight was calculated to be negligible, and it was assumed that any differences in the radiative straggling and multiple scattering of positrons and electrons introduced negligible errors.

### Relative Electron-Proton Scattering Cross Sections

Although this experiment was primarily designed to determine $R$, relative electron scattering cross sections were obtained as a by-product. Absolute cross sections were not directly measured because the mean spectrometer solid angle, averaged over the long target, was not determined. However, absolute cross sections can be derived from the data as follows: We assume that the cross section for the three measurements at $q^2\leq1.3$ F$^{-2}$ is governed by a single form factor $F$, such that $(d\sigma/d\Omega)=F^2(d\sigma/d\Omega)_{\text{point}}$, where $(d\sigma/d\Omega)_{\text{point}}$ is given by the Rosenbluth formula with $F_1=F_2=1$. Furthermore, we use the approximate relation[12] $F=1-(1/6)q^2\alpha^2$, where $\alpha$ is the root-mean-square radius of the proton. Thus, we assume $F$ varies linearly with $q^2$, and the data are normalized to give absolute cross sections by requiring that extrapolation to $q^2=0$ gives $F=1$.

Figure 5 shows the variation of $F$ with $q^2$ for the normalized low momentum-transfer data. The straight-line fit corresponds to $\alpha=0.72\pm0.05$ F, and the data are consistent with other measurements.[13,14] In view of the angles and energies involved here, the variation of $F$ is dominated by $F_1$, and $\alpha$ is thus an estimate of the radius associated with this form factor. The assumption of a straight-line fit to $q^2=1.3$ may not be strictly justified, and thus $\alpha$ is subject to an additional uncertainty. However, the normalization, which is our main concern, depends only on the extrapolation to $q^2=0$ from data at quite small $q^2$ and is thus not very sensitive to reasonable curvature in the dependence of $F$ on $q^2$.

Values of $F^2$ and $d\sigma/d\Omega$, calculated from the relative measurements with the normalization procedure just described, are given in Table II. The uncertainties are estimated random errors for the relative values of the cross sections, including both systematic and statistical uncertainties. Since data at different angles and energies are being compared, the systematic errors are larger than those involved in the determination of $R$. Some new corrections and uncertainties are added, and the energy and angle errors are increased. The latter two in fact dominate the systematic error. The over-all normalization uncertainty, estimated to be 1.5%, is not included in the quoted errors.

The cross section at 130°, 307 MeV, is about 20% higher than that calculated from reference 14. This discrepancy of roughly two standard deviations (considering the uncertainties in reference 14) is not understood. In the determination of $R$, all of the check procedures gave satisfactory results, and we believe the measurement of $R$ to be valid. The discrepancy may have arisen from an undetected error in target location which would change the relative target lengths for 30° and 130° scattering. The cross section for 130° was derived from a normalization to 30°, and such an error would thus produce a discrepancy without affecting the measurements of $R$.

## IV. DISCUSSION

The results given in Table I are shown in Fig. 6, along with calculations of $R$ for potential scattering at 307 MeV in the second Born approximation. The curve labeled $R_{\text{point}}$ is calculated from the formula of McKinley

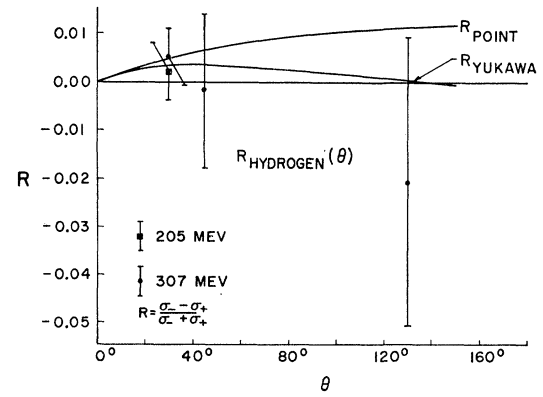


FIG. 6. Comparison of experimental results for $R$ with calculations of potential scattering in second Born Approximation. The theoretical curves are for 307 MeV, but the measurement at 205 Mev is shown for completeness.

[12] R. Hofstadter, Revs. Modern Phys. **28**, 214 (1956).
[13] P. Lehmann, R. Taylor, and R. Wilson, Phys. Rev. **126**, 1183 (1962).
[14] F. Bumiller, M. Croissiaux, E. Dally, and R. Hofstadter, Phys. Rev. **124**, 1623 (1961).

and Feshbach[15] for a point scatterer, while $R_{\text{Yukawa}}$, which applies to scattering from a Yukawa distribution of rms radius 0.72 F, is calculated from the formula given by Lewis.[16] In the absence of anomalous two-photon effects, $R$ is thus expected to be very close to zero. The measured values of $R$ are in accord with this prediction, and the validity of the usual form factor analysis is verified to within a few percent up to $q^2=5.2$, where $q$ is the four-momentum transfer in inverse Fermis.

## ACKNOWLEDGMENTS

It is a pleasure to thank Professor W. K. H. Panofsky for his aid and encouragement during the execution of the experiment, Professor S. D. Drell and Professor Y. S. Tsai for advising us on theoretical matters, and Dr. F. Bumiller for discussions concerning the Faraday cup efficiency and the performance of the rotating coil and the momentum-analyzing systems. The hydrogen target was designed and constructed by E. A. Allton, R. Alvarez, and L. Hand. R. G. Gilbert, L. L. Combs, and T. M. Sartain gave generous assistance in obtaining the positron beam, while L. Boyer, E. Pathway, and J. Grant helped with the construction of much of the apparatus.

## APPENDIX. FARADAY CUP STUDIES

An ideal Faraday cup would have no bias for positrons as compared with electrons, but we consider four effects which can in practice lead to a bias:

1. Asymmetry in the behavior of the electronic integrator when the sign of the beam is reversed.
2. Excess electrons collected by the cup as a result of secondary emission from the entrance window of the vacuum chamber surrounding the cup.
3. Loss of electrons as a result of secondary emission from the cup.
4. Loss of electrons as a result of incomplete containment of the cascade showers produced in the cup material.

We assume the magnitude of effects 2, 3, and 4 to be identical for positrons and electrons, with the bias resulting when a net gain or loss of electrons is added to beam currents of opposite sign. By secondary emission we mean ejection of low-energy electrons by the beam, as in the secondary emission beam monitors described by Tautfest and Fechter.[17]

All of the effects listed above have been investigated experimentally. The integrator bias was found to be negligible in tests performed with a reversible current source. Secondary emission from the entrance window was measured by establishing a weak transverse magnetic field between the entrance window and the cup, as well as by placing a grid behind the entrance window and biasing it to return secondary electrons to the window.[18] In each case, all electrons of less than several hundred eV kinetic energy were prevented from reaching the cup. (Electrons with energy greater than a few hundred eV are known to constitute an extremely small part of the total secondary emission effect.) Both types of measurements gave consistent results, and lead to a bias estimate of $B=+0.0005_{-0.0005}{}^{+0.0006}$, where $B$ is the spurious value of $R$ (i.e., the difference in positron and electron efficiencies divided by the sum) arising from the effect. The two hydrogen ion chambers were used as reference monitors during this and other Faraday cup studies. The asymmetrical error limits result from the fact that this bias cannot be negative. The effect of secondary emission from the cup was evaluated with a grid placed near the bottom of the cup and biased to return all electrons with energies below about 500 eV to the cup. The resulting bias for this effect was $B=-0.0002_{-0.0006}{}^{+0.0002}$.

Brown and Tautfest[8] have discussed the effect of shower penetration in some detail, pointing out that the shower products at the surface of the cup are low-energy gamma rays and the Compton and pair electrons in equilibrium with them. The flux of such gamma rays per incident electron varies almost linearly with beam energy for the high energies of interest here. Thus, to investigate this effect, we have compared the Faraday cup with the ion chambers at 200, 500, and 850 MeV. For such a comparison, it is important to take account of any change in specific ionization with energy, and we have been guided in this by the theory of Budini, Taffara, and Viola.[19]

In contrast to the Faraday cup, the efficiency of the ion chambers is expected to increase with energy. At sufficiently high energies, however, depending upon the density of the gas in the chamber, the specific ionization is expected to be essentially independent of energy. Unfortunately, for our purpose the approximate analytical expressions given by Budini *et al.* are not sufficiently accurate in the region of interest, where the specific ionization is within 1% of its plateau value. We have therefore, during the investigation of shower penetration, attempted to measure this effect by operating the closed chamber at two atmospheres, while the flow chamber was, as usual, at one atmosphere.

With respect to the flow ion chamber, the Faraday cup efficiency decreased by $(-0.37\pm0.08)\%$ from 200

[15] W. A. McKinley, Jr., and H. Feshbach, Phys. Rev. **74**, 1759 (1948).
[16] R. R. Lewis, Phys. Rev. **102**, 537 (1956).
[17] G. W. Tautfest and H. R. Fechter, Phys. Rev. **96**, 35 (1954).
[18] Secondary emission effects have, in the past, been investigated by applying a variable bias voltage between the cup and vacuum chamber (see, for example, reference 8). A "bias curve" of efficiency as a function of the magnitude and polarity of this voltage is measured, and the extreme variation exhibited by this curve is used to infer limits (typically ~1%) on the net gain or loss of electrons by the cup. Spuriously large efficiency variations tend to occur as the result of enhancement of one secondary emission effect when the bias is set to eliminate another. This type of investigation is thus useful only in establishing a rather extreme upper limit, and it has not sufficed for our purposes.
[19] P. Budini, L. Taffara, and C. Viola, Nuovo cimento **18**, 864 (1960).

to 850 MeV. With respect to the closed chamber, the efficiency change was $(+0.03\pm0.11)\%$ for the same energy range. A plausible interpretation of these results is that the Faraday cup efficiency decreased by less than about 0.1% in going from 200 to 850 MeV, while the specific ionization of hydrogen at 200 MeV is within about 0.4% of its plateau value at one atmosphere and within about 0.1% at two atmospheres. Assuming linearity, this leads to a shower penetration bias of $B=0.0000_{-0.0004}{}^{+0.0000}$, at 300 MeV. If this interpretation is rejected and if both ion chambers are given equal weight and their results averaged, the estimated bias would be $B=-0.0006_{-0.0003}{}^{+0.0000}$. From these considerations we have assigned a bias of $B=0.0000_{-0.0010}{}^{+0.0000}$, where the added uncertainty allows for the second alternative.

Combining the determinations of the various Faraday cup biases, the final result for the net bias is

$$B=0.0000\pm0.0015,$$

at 300 MeV. This also implies that the absolute efficiency of this monitor is $(100.00\pm0.15)\%$ at this energy. All of the factors which have been studied experimentally can be estimated rather roughly, and the experimental results are consistent with such estimates.

PHYSICAL REVIEW VOLUME 128, NUMBER 4 NOVEMBER 15, 1962

# Search for Multipion Resonances in the Reaction $\bar{p}+p \rightarrow 3\pi^+ + 3\pi^- + n\pi^0$†‡

NGUYEN-HUU XUONG* AND GERALD R. LYNCH
*Lawrence Radiation Laboratory, University of California, Berkeley, California*

(Received July 13, 1962)

We report here the study of the reaction $\bar{p}+p \rightarrow 3\pi^+ + 3\pi^- + n\pi^0$ at 1.61 BeV/$c$ ($E_{c.m.}=2.290$ BeV), with the aim of detecting multipion resonances in the final states.

The experiment was performed in the Lawrence Radiation Laboratory's 72-in. liquid-hydrogen bubble chamber. The total number of six-prong events in the sample is 715. The events were measured with the Franckenstein measuring projector. The events were analyzed by using the PANG, KICK, and EXAMIN programs with IBM 704, 709, and 7090 computers.

The cross sections of various processes are found to be: $\sigma(\bar{p}+p \rightarrow 3\pi^+ + 3\pi^-)=1.16\pm0.1$ mb, $\sigma(\bar{p}+p \rightarrow 3\pi^+ + 3\pi^- + \pi^0)=1.8\pm0.25$ mb, $\sigma(\bar{p}+p \rightarrow 3\pi^+ + 3\pi^- + 2\pi^0)=1.05\pm0.25$ mb. The angular distributions are symmetrical for all three types of events.

The existence of the $\omega$ meson ($T=0$ three-pion resonance at 780 MeV) is further confirmed. With the hypothesis of $G$-parity conservation in the decay process (strong decay), the spin and parity of the $\omega$ meson is confirmed as $1^-$ by the Dalitz-plot method. Even with the hypothesis of $G$-parity nonconservation in the decay process (electromagnetic decay), the $1^-$ spin-parity assignment is still strongly suggested by the small values of the ratios of $R[(\omega \rightarrow 4\pi)/(\omega \rightarrow \pi^+\pi^-\pi^0)]$ and $R[(\omega \rightarrow \text{neutral})/(\omega \rightarrow \pi^+ + \pi^- + \pi^0)]$. We do not observe any $T=0$ three-pion resonance at 550 MeV ($\eta$ meson). The neutral four-pion effective mass $M_4$ distribution shows a suggestive peak at 1.04 BeV.

The distribution of the two-pion effective mass $M_2$ of the $\bar{p}+p \rightarrow 3\pi^+ + 3\pi^-$ events shows a big difference between $|Q|=2$ (for like-pion pairs) and $Q=0$ (for unlike-pion pairs) at the low-value region of $M_2$. At this region the $M_2$ distribution of like-pion pairs lies above that from phase-space calculations, and the one of unlike-pion pairs is well below. We tentatively attribute this effect to the Bose-Einstein effect on the pions.

The ratio $R[(\rho^\pm \rightarrow \pi^\pm + \eta \text{ followed by } \eta \rightarrow \pi^+\pi^-\pi^0)/(\rho^\pm \rightarrow \pi^\pm\pi^0)]$ is determined to be $1.2\pm2.0\%$. This small ratio agrees with $0^{-+}$ assignment for spin, parity and G parity of the $\eta$ meson, but cannot rule out the $1^-$ possibility. Upper limits of some other decay rates of $\rho$ and $\omega$ mesons are presented.

## I. INTRODUCTION

IT is a little paradoxical that a search for more resonances or unstable particles can be introduced by a theory that tries to reduce the fundamental particles to three: the "Eightfold Way" Theory.[1]

In this theory Gell-Mann, using the Sakata Model[2] with only three fundamental particles $p$, $n$, $\Lambda$ (and their antiparticles $\bar{p}$, $\bar{n}$, $\bar{\Lambda}$), and supposing that mesons are formed of fundamental baryons and their antiparticles interacting via a "gluon," predicts the existences of two sets of mesons, the pseudoscalar set of $0^-$ mesons (spin $=0$, parity odd) and the vector set of $1^-$ mesons (spin 1, parity odd). Each set is divided into a singlet and an octet. He also conjectures the existence of the scalar $0^+$ and $1^+$ axial-vector mesons. These mesons are shown in Table I.

The decay of these proposed particles is governed by the conservation laws of strong (or electromagnetic) interactions. Here we are mostly interested in nonstrange particles ($S=0$). Table II shows the prediction of the decays of these particles.

Though the mesons presented in Table II include all possible combinations of spin, isotopic spin, and parity with neither spin nor isotopic spin exceeding unity, they represent only half of the possible states

† Work done under the auspices of the U. S. Atomic Energy Commission.

‡ Based on work submitted by N.H.X. to the Graduate Division of the University of California in partial fulfillment of requirements for the degree of Doctor of Philosophy.

* Present address: Physics Department, University of California, at San Diego, La Jolla, California.

[1] M. Gell-Mann, California Institute of Technology Synchroton Laboratory Report No. CTSL-20, 1961 (unpublished); Phys. Rev. **125**, 1067 (1962).

[2] S. Sakata, Progr. Theoret. Phys. (Kyoto) **16**, 686 (1956).